FIZYKA BUDOWLI W TEORII I PRAKTYCE
TOM IX, Nr 1 – 2017

Instytut Fizyki Budowli

PARTICLE SIZE CHARACTERISATION OF SCMs BY MERCURY INTRUSION POROSIMETRY

Agnieszka J KLEMM[1*], David E. WIGGINS[2]

[1]*Glasgow Caledonian University, School of Engineering and Built Environment, 70 Cowcaddens road, G4 0BA, Glasgow, UK, e-mail:a.klemm@gcu.ac.uk*
[2]*Curtins Consulting (Kendal), Kendal, UK*

Summary: Mercury intrusion porosimetry (MIP) is widely used for the microstructural characterisation of porous solids. Comparatively few studies have employed the technique to characterise the size of particles within powdered samples. The present study uses the MIP technique to characterise the particle sizes of contemporary supplementary cementitious materials (SCMs), and in particular uses the technique to present particle size distributions, rather than a single mean size. Representivity of the technique for known limitations of non-spherical and porous particles are checked using the Scanning Electron Microscope. The findings indicate that the MIP affords a good approximation of particle sizes, including distributions, of spherical and non-spherical particles. The technique was also found to provide reasonable accuracy for estimating the particle sizes of highly porous particles, where distinction between inter-particle and intra-particle porosity was made**.**

Keywords: particle size distribution; mercury intrusion porosimetry; supplementary cementitious materials.

1. INTRODUCTION

Particle size is closely related to the reactivity of supplementary cementitious materials (SCMs). Industrial by-products, their partial replacement of cement in concrete mixes represents a substantial offset to the consequent environmental impact. Furthermore, a wide range of concretes optimised for specific applications are now possible with SCMs. With industrial production comes the need for efficient quality control analyses; this time-orientated credential is met by mercury intrusion porosimetry (MIP).

A suite of particle characterisation methods is available, each with strengths and weaknesses which vary according to the actual sample properties: SCMs, for example, are typically by-products of specific industrial processes, and by their nature present varied characteristics. The suite includes Blaine (air-permeability), BET, image analysis, laser diffraction, sieving and MIP. A state-of-the-art review of SCM particle characterisation methods was undertaken by Arvaniti et al. [1], which included the MIP technique, and found it to represent a valuable contribution to the suite of characterisation techniques. Particular strengths aside from the speed of the MIP technique include: no need for prior particle dispersion; a 3-dimensional representation of the sample; little prior knowledge of the studied sample; a 'one-size' instrument calibration, and an ability to probe down to the nano-metre size of pore or particle. The latter is an especially important strength of particle characterisation technique [2].

Mercury intrusion porosimetry relies on the premise that the pressure required to force mercury (eminently non-wetting fluid) through an opening in a given material is a function of the size of that opening, and the surface chemistry of that material. Particle size characterisation through MIP applies this to a model assuming packed spheres of a given size and packing geometry [3]

2. THEORETICAL FOUNDATIONS

The present study adopts the Modified Mayer-Stowe method. The particle size diameter is derived from the premise that the breakthrough pressure equilibrates with a function of the particle size and packing arrangement of those particles (Eqn. 1). KMS is the Mayer-Stowe proportionality constant, descriptive of packing arrangement

$$D = \frac{2 \cdot K_{MS} \cdot \gamma}{P_b} \qquad (1)$$

*Autor korespondencyjny, e-mail: a.klemm@gcu.ac.uk

Where the original work by Mayer-Stowe (1965) provided an estimate of the equivalent monosized spherical particle size, modern porosimeters idealise the sample and apply the expression to each point on the intrusion curve, to obtain an approximation of distribution across different particle sizes. Importantly, for this function it must first deduce and assign KMS as constant for each point on the intrusion curve.

KMS is derived from the total intrusion volume (i.e. the interstitial volume, assuming non-porous particles). Packing arrangement of monosized spheres can vary in interstitial porosity from the densest (triangular) 25.95% to the most porous (square) 47.64% configurations (Fig 1, a). Application of the packing geometry is schematically shown in Fig. 1 (b)

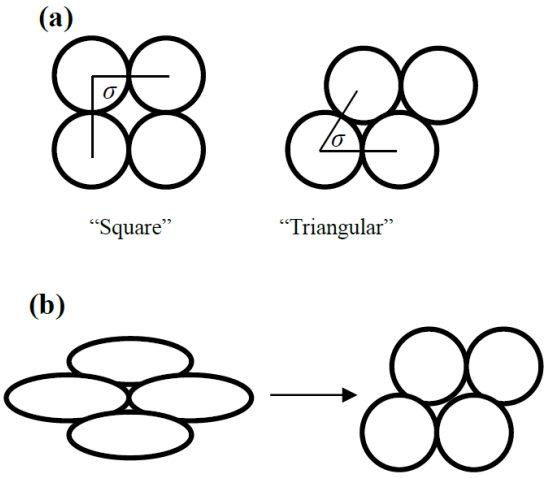

Fig. 1. (a) Packing geometry considered in the assignation of KMS; (b) Schematic application of packing arrangement to non-spherical particles.

KMS is then interpolated from the Mayer-Stowe tables, drawing upon the θadv as the advancing contact angle; and ϵinterstitial as the interstitial porosity. The Mayer-Stowe tabular computations for various packing configurations (Table II, (3)) are then converted into interstitial porosities using Eqn. 2, where σ is the packing angle

$$\epsilon = 1 - \frac{\pi}{6}\sqrt{(1 - 3cos^2\sigma + 2cos^3\sigma)} \qquad (2)$$

The advancing contact angle, θadv, is a required input, here employed at 130°. Thus, KMS can now be found through feeding θadv and ϵinterstitial. Once KMS is assigned, the only variable is now the applied pressure, and the equivalent particle diameter for the respective pressure is returned, and a distribution can be approximated.

In order to obtain particle size distributions, KMS must be set as constant across each point on the intrusion curve, because the envelope volume can only be determined for the bulk sample (using the Archimedes principle), i.e. once the high-pressure intrusion is concluded. Whilst the incremental pressure is measured, and the incremental intrusion volume is also measured, there is no means of deducing the envelope volume occupied by that respective intrusion. Therefore the interstitial porosity cannot be determined on an incremental basis. The consequence of this is that it forces a self-similarity relationship between the packed-bead model on the macro and micro scales, which is not perhaps met in practice, as observed by Mathews [4].

The error introduced here can perhaps be considered in the same vein as that of decreasing pore radii in the conventional MIP deduction of pore size distributions. In the case of powders where there exists a distribution of particle sizes which allows fines to occupy the interstices between larger particles (Fig. 2, Fig. 3), the particle arrangement is first idealised to an arrangement of monosized spheres whose packing arrangement and size best fits the intrusion volume. This has the effect of averaging the sample by volume (Fig. 2)

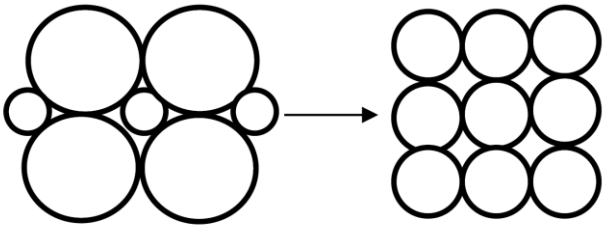

Fig. 2. Representation of mean particle size derived from total interstitial porosity for graded particle arrangements

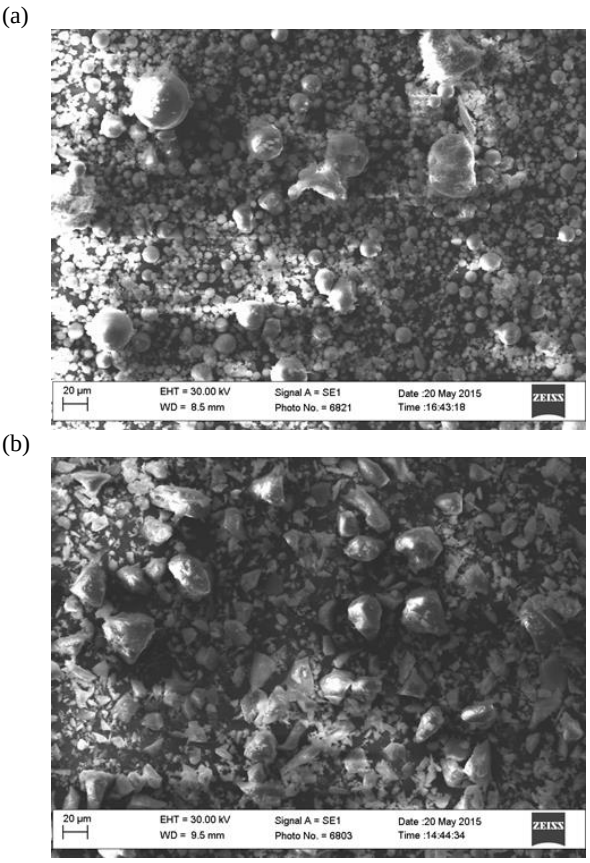

Fig. 3. SEM micrographs comparing spherical and non-spherical particles for study under MIP. (a):Fly ash; (b): Slag

Another consequence of the above KMS derivation from the total intrusion volume is that any intraparticle porosity (spaces within particles) then affects the packing angle, to an extent, which would vary on the relative difference between inter- and intra-particle pore sizes (Fig. 4). However for powder samples, it may be expected that whilst their interparticle voids may be high (spaces between particles), their intraparticle voids (spaces within particles) are typically small. Deduction of intraparticle porosity may be expected to be made through any inflection late in the intrusion curve, towards the higher pressures

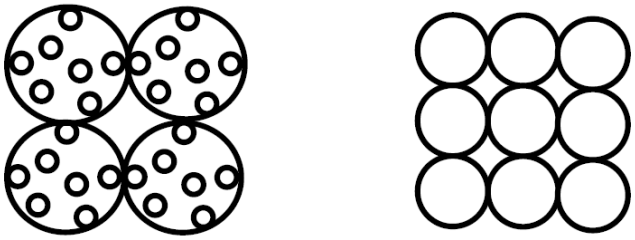

Fig.4. Representation of samples exhibiting significant intraparticle porosity

The idealisation of the sample to permit derivation of KMS, and the assignation of KMS to each point on the intrusion curve, both carry a degree of intrinsic error [5]. Nevertheless a distribution of particle sizes can be obtained with good agreement with complementary analyses under different methods, especially those with narrow ranges of particles exhibiting monomodal distribution [6].

Stanley-Wood (1979) used MIP to study the distributions of three different powders, comprising non-porous, microporous and meso/macro-porous particles respectively. Good agreement was found for the non-porous powders when compared with 'conventional' characterisation techniques. The presence of intraparticle porosity was able to be determined in the case of the microporous particles, however the particles with meso/macro-porosity bore little relation to the results of other characterisation techniques [7].

Svata & Zabransky (1969/70) studied the distributions of four different powders of known particle grading (each was specifically manufactured), and in all cases found good accuracy from the MIP analysis (8). Orr (1969/70) reported good agreement between the findings of an MIP analysis with that of a Coulter Counter [9].

The obtained "Particle Size Distribution" is perhaps better termed the "Equivalent Spherical Size Distribution", as the modelled set of spheres which best represents the logged experimental data [10]. Representivity is rather dependent upon how similar the particle geometry is to that of a set of spheres; plate-like, or very angular, or wide ranges of particles conform less to the intrinsic model than monosized well-rounded particles [11].

3. EXPERIMENTAL WORK

SCMs elected for the study of particle size distributions were namely cement (CEM II), fly ash, slag, lime (NHL 3.5), and silica fume. The materials were characterized initially in isolation of one another, each found to comprise fairly monosized particle arrangements. They were then appraised for agreement with other techniques. Selected samples were then blended with each other in varying proportions, to gauge the suitability of the analysis technique for the characterization of graded powder materials (comprising a broader particle size distribution). If the predominant particle size as identified in isolation could be reflected in the study of the blended samples, this would indicate suitability of the technique.

Blending of the above was undertaken on a proportion-by-weight basis, the respective bulk batch then manually shaken in a sealed container to intersperse the different materials. All samples were oven-dried at 75°C for a period of one hour prior to analysis, and then acclimatized in a desiccator for approximately15mins to minimize moisture absorption from the environment during cooling. The characterization instrument was the AutoPore IV Mercury Porosimeter from MicroMeritics. Intrusion is stepwise, in fine increments. The data reduction package employs the Modified Mayer-Stowe theoretical background, as above described.

To investigate the issue of characterising particles featuring intraparticle porosity, cenospheres were introduced to the study, and were examined under MIP and under the Scanning Electron Microscope (SEM), to ensure accurate distinction of particle size and particle porosity from the MIP intrusion volumes. The instrument used in this regard was the Carl Zeiss EVO 50 model

4. RESULTS AND ANALYSIS

The powders of cement, fly ash, slag and dry-hydrate lime all exhibit very close, repeatable particle arrangements of narrow ranges occupying some 5,000-10,000nm (Fig.4a-d). Each intrusion graph represents two analyses (solid and dashed lines). This similarity is unsurprising, in view of the production process of finish milling shared by cement, slag and lime [12]. Nominal intrusion within the larger particle size range was experienced for each of the foregoing. A base pressure of 0.5psia is applied to 'zero' the analysis (filling voids of 360μm and above), to fill the interstices around the bulk sample. It is conceivable, however, that the intrusion in advance of the breakthrough is attributable to compression of the bulk sample under preload, and the filling of air pockets. Unlike in the study of porous solids, the particles of the powder are not cemented in place relative to each other.

The distinct peak exhibited by each of the samples represents the 'breakthrough pressure', according directly with the original Mayer-Stowe model, which relates the pressure at breakthrough to an equivalent mean spherical size. Intrusion at the breakthrough inflection represents the predominant size of the particles.

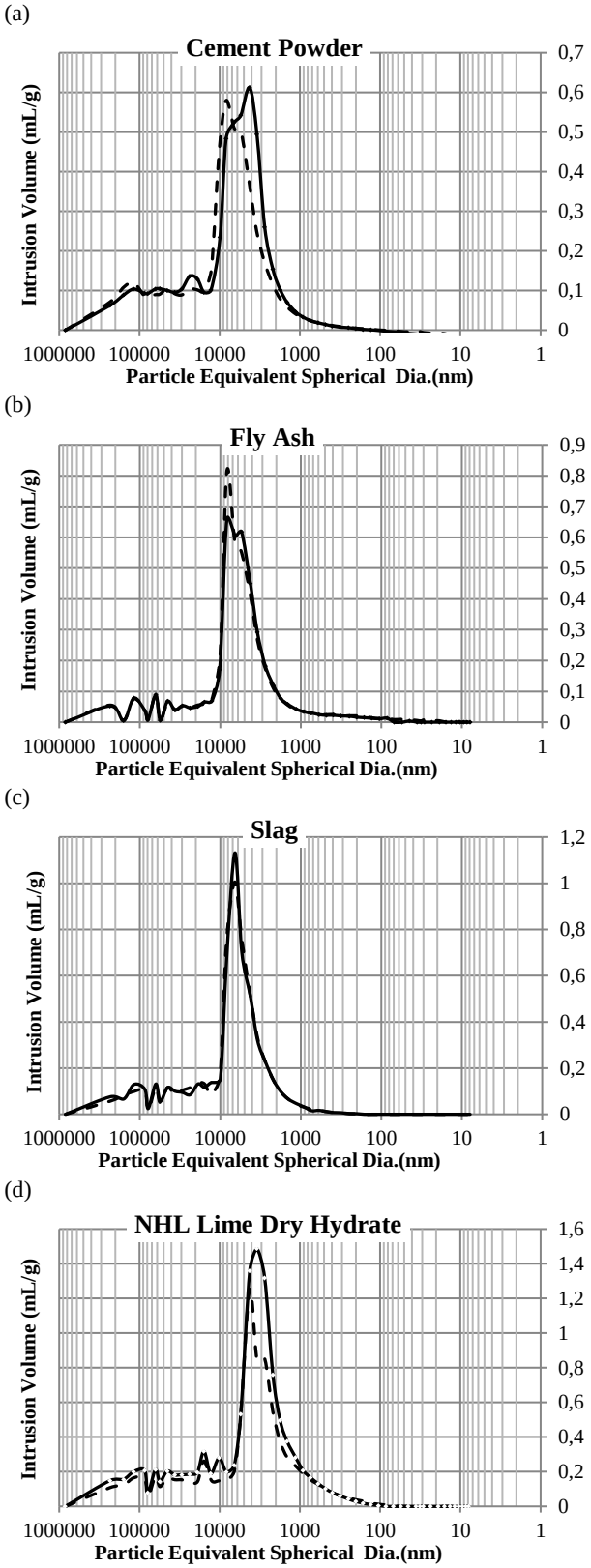

Fig.4 (a-d). Particle size (equivalent spheres)

The distinctly smaller particle size of the silica fume (Fig.5) reflects the different material origin. It is two orders of magnitude (a factor of 100) finer than cement powder. Owing to its fineness (in addition to its mineralogy), it is an extremely reactive pozzolan.

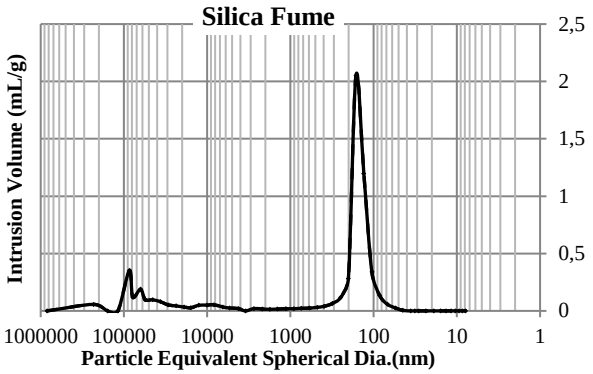

Fig.5: Particle size (equivalent spheres) of silica fume.

The distinct intrusion peaks representing the predominant particle size of the above powder materials is in general accord with the literature [13]. Studies on silica fumes have found a broad range of particle sizes when the sample remains agglomerated [14], however the size of the individual particles (dispersed) agrees with the present findings for MIP, around 150nm. Evidentially, the MIP technique disperses the agglomerated particles during analysis.

A high level of repeatability is indicated by the above analyses, for studying the powders of relatively narrow size range so far discussed. In order to gauge how the MIP technique would perform in returning a representative distribution of particle sizes for a graded sample, selected samples with known predominant particle size were blended together (Fig.6). Comparisons between individual materials are presented in Table 1. As anticipated the blending of materials of very comparable particle size, despite different particle shape, returned a result which matched the individual analyses. Powders with similar particle size blended together, representing monomodal intrusion (Fig.6b)

Table 1. Comparison of SCM particle sizes from [13]

SCM	Sieve Analysis (nm)	Laser Diff. (nm)	MIP (nm)
Fly Ash	< 50,000	10,000 - 15,000	5,000-10,000
Slag	< 50,000	6,000 – 10,000	5,000–10,000
Silica Fume	-	400	150

(a)

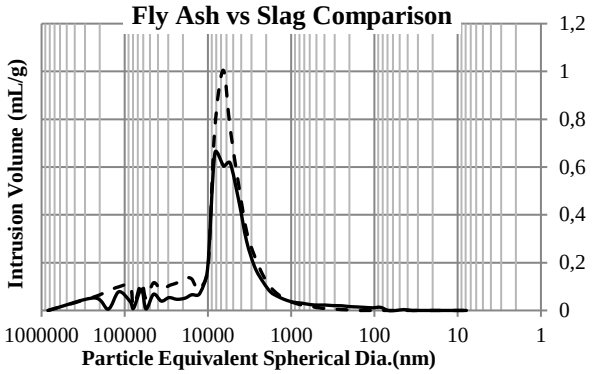

(b)

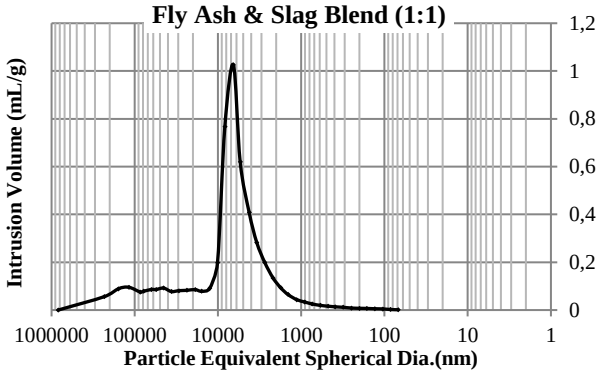

Fig.6 (a-b). Overlay comparison of fly ash (solid line) and slag powders (dashed line) isolation (a); Particle size (equivalent spheres) of an equal blend of fly ash and slag (b).

The blending of powders with different particle sizes returned an insight as to the suitability of the MIP technique to study samples comprising graded particle arrangements. The overlay of fly ash and silica samples (Fig.7a) did not directly accord with the blend of those samples (Fig.7b), although common traits were depicted. Intrusion peaks within the known particle size ranges were recorded in the blend, for the fly-ash constituent at 5,000-10,000nm, and for the silica-fume at some 100-200nm. However the respective peaks are bridged by intermediate intrusion, suggesting particle sizes, which are known to be absent, i.e. those around 1,000nm.

The degree of bridging between the peaks was investigated by varying the constituent proportions in the blends, in both directions from the equal weighting (Fig.8a-b). As expected, the peak corresponding to the dominating constituent reflected the change in interstitial porosity of the bulk blend (note the change in the height of the silica-fume peak). Notably, the "false peak" between the fly-ash and silica-fume peaks appeared to reflect the constituent proportional change. This "false peak" was more pronounced for the blend with higher proportion of smaller particle (silica fume), and less pronounced where the weighting was towards the larger particle (fly ash).

(a)

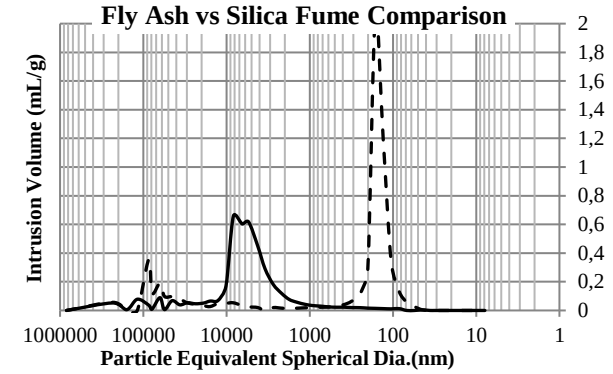

(b)

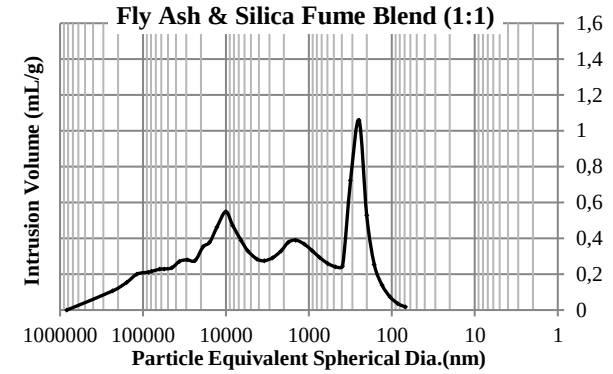

Fig.7 (a-b). Overlay comparison of fly ash (solid line) and silica fume (dashed line) powders in isolation (a); Particle size (equivalent spheres) of an equal blend of fly ash and silica fume (b).

Fine sand, sieved to pass 63μm sieve, was introduced into the blend firstly with fly ash (Fig.8c) and then together with fly ash and silica fume (Fig.8d). The intrusion peaks of the fine sand and the fly ash were not fully blended (Fig.8c) before the inclusion of further fines by the addition of silica fume, likely clogging the interstices (Fig.8d).

(a)

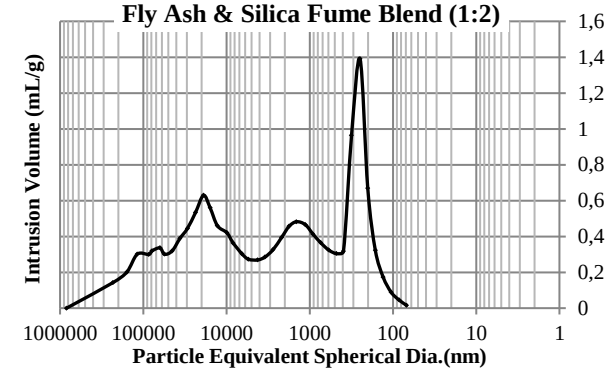

(b)

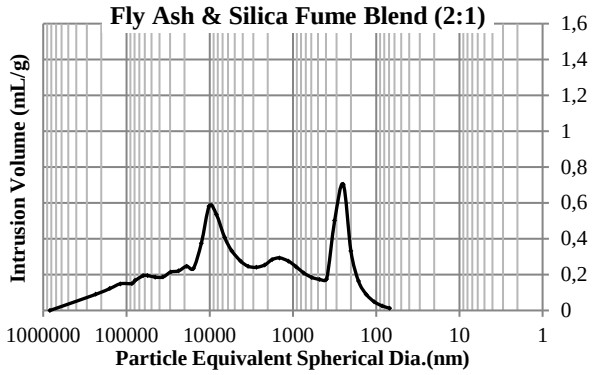

(c)

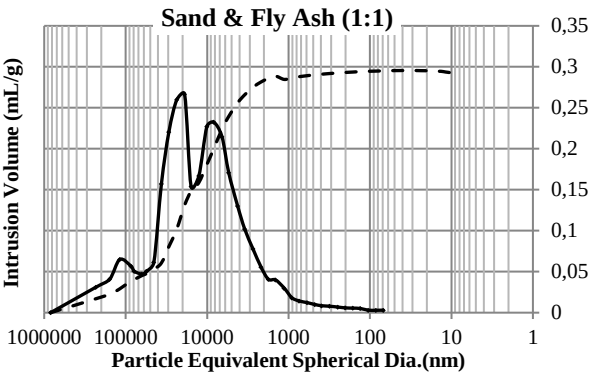

(d)

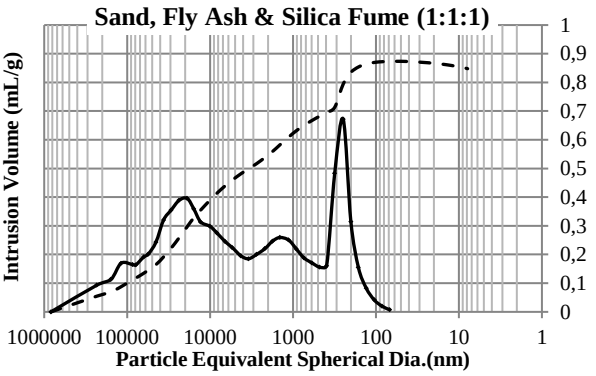

Fig.8 (a-d): Particle size (equivalent spheres) of a blend of fly ash and silica fume, weighted towards silica fume
(a); Particle size (equivalent spheres) of a blend of fly ash and silica fume weighted towards fly ash (b); Particle size (equivalent spheres) of an equal blend of fine sand and fly ash with cumulative intrusion overlay shown dashed (c) Particle size (equivalent spheres) of a blend of fine sand, fly ash and silica fume with cumulative intrusion overlay shown dashed (d).

The false-peak phenomenon was investigated further: the magnitude of the gap between the respective known particle sizes was increased, by blending fine sand (sieved to pass 63µm) with silica fume, in equal proportion (Fig.9a). The predominance of the "false peak" increased. The "false peak" appears to record intrusion through the interstices between the large particles, which are partly clogged with fines from the smaller particles (Fig.9b). The false peak increases in prevalence with an increase in the proportion of fines within the sample. Curiously the location of the false peak did not change with increasing the gap between the sizes of the two constituent materials: it remained centred on 1,000nm

(a)

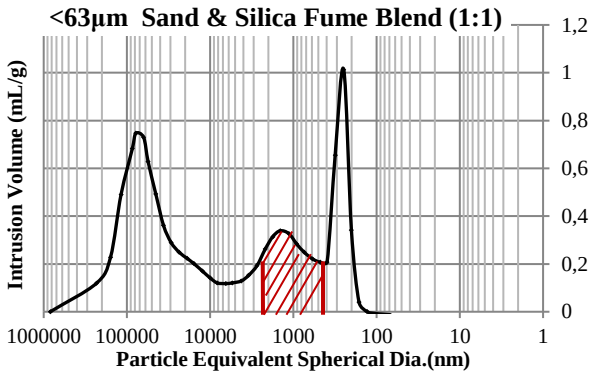

(b)

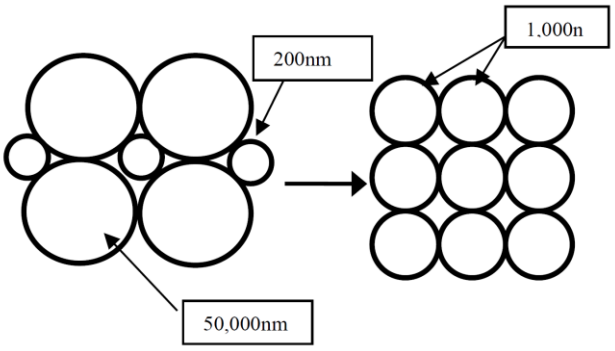

Fig.9(a-b): Particle size (equivalent spheres) of a blend of fine sand and silica fume, equally weighted (a); Schematic representation of the false peak error induced (b).

Samples with intraparticle porosity are known to present issue (7); an assumption of the MS model is that particles are non-porous (Fig. 4). Nevertheless, Leon (6) demonstrated distinction between inter- and intra- particle porosity can be made from the intrusion data. An emerging SCM, the lightweight fine filler 'cenosphere', was studied. Cenospheres are spherical in shape with high intraparticle porosity. The particle size characterisation is presented in Fig.10 (a-b), and the results validated under the SEM in Fig 10 (c-f)

(a)

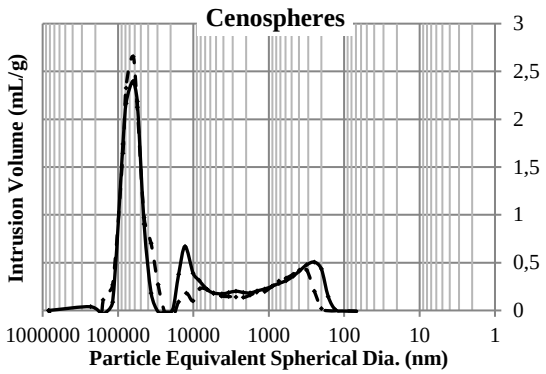

(b)

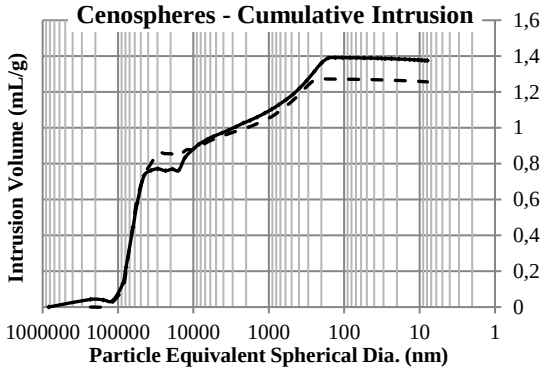

(c)

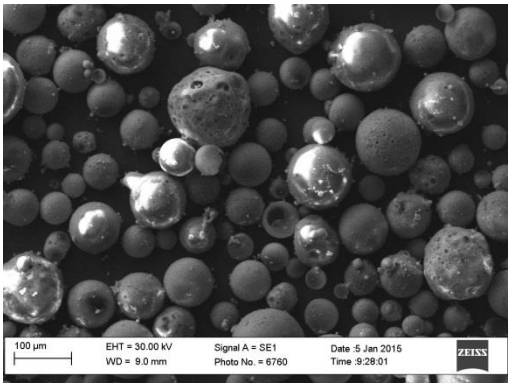

(d)

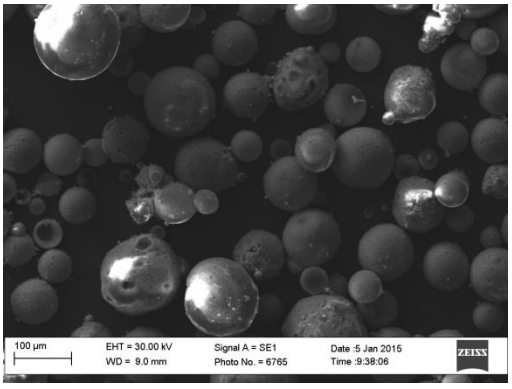

(e)

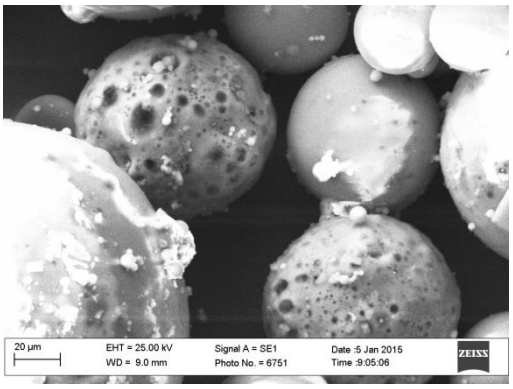

(f)

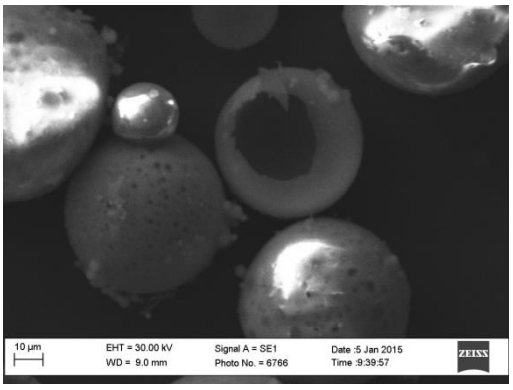

Fig.10 (a-f). Cenospheres particle characterisation. a) Differential intrusion (distribution); b) Cumulative intrusion, showing secondary inflection on intraparticle intrusion; c-d) SEM micrographs of particle distribution; e-f) SEM micrographs of particles showing intraparticle porosity

The particle size distribution derived from the MIP data (Fig.10a) presents a bimodal distribution, firstly with a distinct peak representing particle sizes ranging from some 150µm down to some 30µm. The cenospheres sampled are reported by the manufacturer as ranging from 150µm to 50µm, and there is agreement between the ranges. This range is represented on the cumulative intrusion curve (Fig.10b), at the steep inflection corresponding to the initial breakthrough. The size distribution declared by the manufacturer and as represented in the MIP data initial intrusion was validated under the SEM (Fig.10c-d), again with close agreement.

A secondary intrusion is observed in the distribution (Fig.10a). This does not relate to interstitial intrusion or particle size; the secondary intrusion represents intraparticle porosity. Inspection of this secondary intrusion can be made from the cumulative intrusion graph (Fig.10b), as a late inflection after initial intrusion was exhausted. Figure 10 (e-f) demonstrate the high intraparticle porosity, which is accessible from the surface of the cenospheres. In view of the validation provided by the SEM micrographs, deduction of intraparticle intrusion can be made from the MIP data. The intraparticle intrusion volume should be ignored (in the

context of particle size characterisation, but could readily be used to estimate intraparticle porosity for the mean particle size). Furthermore, with the revised total intrusion volume, the packing configuration would then require correction, and KMS reassigned. However in the present case with the cenospheres, the MIP particle size estimate (the initial breakthrough intrusion) represents reasonably good agreement with the particle size observed under the SEM, and adjustment of KMS has not been made.

4. CONCLUSIONS

1. MIP returns a fast, repeatable and cross-comparable result for characterising the particle size of powdered materials of fairly monosized particle arrangement, probing down to the nano-level.
2. The steepest inflection on the intrusion curve affords the closest representation of the predominant particle size for the bulk sample, closely according with the original MS model.
3. Presentation of the MIP data in particle size distribution format is useful for determining whether or not there is a distribution, or whether the particles are monosized (an important conclusion in its own right), and in so doing inferring the degree of accuracy of the MIP technique, or indeed directing towards the appropriate selection of other technique(s).
4. MIP for characterising the particle size distribution of graded materials forces an error which appears to be associated with fines clogging the interstices between larger particles. Applicability of the technique then seems to be limited to studying graded distributions of known constituent materials (with known particle sizes): in such case it would merely identify the presence of a certain material.
5. In the characterisation of porous particles, distinction can be made between inter-particle and intra-particle intrusion, especially where supplementary analyses such as examination under the SEM are undertaken.

ACKNOWLEDGEMENTS

The authors would like to thank Steve Coulson of MicroMeritics UK for the contribution on the theoretical principles underlying particle size characterisation by the MIP method. Furthermore, we would like to thank ScotAsh Ltd. and Hanson Heidelberg Cement Group for their continued support in providing the sample materials.

References:

[1] Arvaniti EC, Juenger MCG, Bernal SA, Duchesne J, Courard L, Leroy S, et al. Physical characterization methods for supplementary cementitious materials. Materials and Structures 2014.
[2] León CA. Particle size distribution of carbon blacks by mercury porosimetry. Rubber Chemistry and Technology 1998;71(5):988-997.
[3] Mayer, R.P. & Stowe, R.A. Mercury porosimetry: breakthrough pressure for penetration between packed spheres. Journal of Colloid Science 1965;20:893-911.
[4] T. J. Mathews. Void structure, colloid and tracer transport properties of stratified porous mediaUniversity of Plymouth; 1999.
[5] Huggett S, Mathews P, Matthews T. Estimating particle size distributions from a network model of porous media. Powder Technology 1999;104:169-179.
[6] León CA. New perspectives in mercury porosimetry. Advances in Colloid and Interface Science 1998;76-77:341-372.
[7] Stanley-Wood N. Sub-micrometre Particle Size Characterisation and Distribution by Mercury Penetration. The Analyst 1979;104(1235):97-105.
[8] Svata, M. & Zabransky, Z. Comparison of Mercury Porosimetry, Sedimentation and Microscopy for Determining the Grain Size Distribution of Powdered Particles. Powder Technology 1969/70;3:296-298.
[9] Orr C. Application of Mercury Penetration to Materials Analysis. Powder Technology 1969/70;3:117-123.
[10] Webb PA. An Introduction To The Physical Characterization of Materials by Mercury Intrusion Porosimetry with Emphasis On Reduction And Presentation of Experimental Data. 2001.
[11] Webb PA&O, C. Analytical methods in fine particle technology. Norcross: Micromeritics Instrument Corporation; 1997.
[12] Darling P. Clinker grinding. Rock Products 1997.
[13] Arvaniti EC, Bernal SA, Courard L, De Belie N, Duchesne J, Juenger MCG, et al. Determination of particle size, surface area, and shape of supplementary cementitious materials by different techniques. Materials and Structures 2014.
[14] Diamond, S. & Sahu, S. Densified silica fume: particle sizes and dispersion in concrete. Materials and Structures 2006;39:549-859.